JOURNAL OF AVIATION

e-ISSN: 2587-1676 J Aviat 2020; 4(2): 36-47

Research Article DOI : 10.30518/jav.787455

Fundamental Frequency Optimization of Doubly Curved Aerospace Structural Panels via Variable Stiffness Concept

Touraj FARSADI[1*], *Hasan KURTARAN*[1]

Adana Alparslan Türkeş Science and Technology University, Adana, Turkey.

ABSTRACT

The fundamental natural frequencies of curvilinear fiber composite doubly curved panels are optimized. Doubly curved panels are used in numerous components of the structural frames of aerospace vehicles. The variable stiffness performance is achieved by changing the fiber path to the curvilinear fiber path function in the composite structures. The structural model is developed based on the virtual work rule. The target is to attain the best fiber paths with maximum fundamental frequencies. An eight-layer composite doubly curved panel with two forms of boundary conditions is considered as an example in this research. The boundary conditions include; CCCC, FCFC. Von-Karman kinematic strain relations are utilized and the FSDT is used to generalize the equation for the doubly curved panel. Generalized Differential Quadrature (GDQ) theory of solution is applied to solve the differential governing equations of motion. Numerical results reveal the efficiency of the curvilinear fiber path concept on the frequencies of the doubly curved panel. The optimum fiber path function of each layer is offered for the free vibration study.

Keywords: Doubly Curved Panel, Curvilinear Fiber Path, Generalized Differential Quadrature, Free Vibration, Optimization

1. Introduction

It is interesting to design laminated panels of aerospace structures using curvilinear fibers instead of unidirectional ones, since by using a Variable Stiffness Composite Laminate (VSCL) the natural frequencies change, and vibrational resonance can be avoided [1]. The automated manufacturing of composite laminates allows panel fiber hardening to become an achievable and viable approach for weight reduction and structural performance enhancement in aircraft structures. With the wide use of composite fibers and automated fiber placement manufacturing technology for composite structures, the variable stiffness architecture has become more interesting for large scale applications in aircraft structures, and structural performance improvements in helicopter and missile applications. The vibration performance can be improved by tailoring the fiber path of different

Corresponding Author: Touraj FARSADI tfarsadi@atu.edu.tr

Citation: Farsadi T., Kurtaran H. (2020) Fundamental Frequency Optimization of Aerospace Structure Doubly Curved Panel via Variable Stiffness Concept J. Aviat. 4 (2), 36-47.

ORCID: [1*] https://orcid.org/0000-0002-9363-3805; [2] https://orcid.org/0000-0002-2552-8616

DOI: https://doi.org/10.30518/jav.787455

Received: 28 August 2020 **Accepted:** 26 December 2020 **Published (Online):** 28 December 2020

layers. Laminated composite doubly curved panels are used as the main components in aerospace industries (see Figure 1).

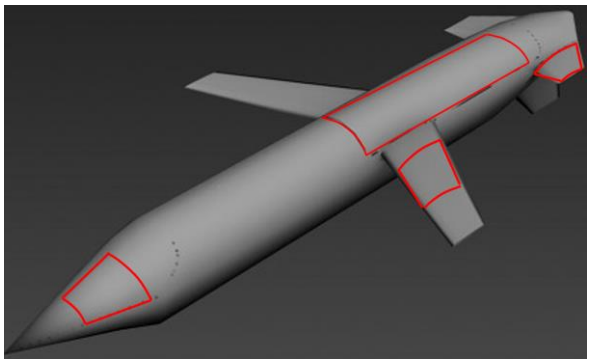

Figure 1 Laminated composite skew and taper curved panels used in a missile structure

The buckling and free-vibration experiments and study were performed by Ref [2] on constant and variable stiffness CFRP cylinders. Narita and Robinson [3] applied the Ritz based method for layer optimization of thin cylindrical laminates in order to maximize the frequencies. Serhat and Basdogan [4] optimized the fundamental frequency of panels in the lamination parameter domain via an optimization structure using the FE method. The research presented by Blom [5] and Blom et. at. [6,7] examine the fundamental natural frequencies of VSCL from flat panels to conical and cylindrical shells by means of numerical and experimental approaches. Structural studies are performed applying the FE program ABAQUS.

Honda et al. [8] offered an optimization method to optimize frequencies however minimizing the curvatures of fibers. Tornabene et al. [9] investigated the vibration characteristics of doubly-curved panels strengthened by the variable stiffness method. A sensitivity study done by Zhao et al. [10] showed that altering fiber functions can increase the frequencies of the plates. Wu and Lee [11] explored the frequency behavior of a conical shell through the curvilinear fiber concept, and attained varies of 7% and 20% in the first natural frequencies of panels with CCCC and SSSS boundary conditions, respectively. The maximization of the fundamental frequency of a composite cylindrical shell using a curvilinear fiber path is addressed by Luersen et. al. [12]. The fiber path equation parameters are optimized using a surrogate-based methodology. Hao et. al. [13] presents the buckling study for curvilinear fiber panels utilizing a combined procedure of exact modeling, isogeometric theory, and optimization for curvilinear fiber composite rectangular panels.

The optimum lay-up design for the maximum first natural frequency of VSCL plates is examined by a layerwise optimization procedure by Houmat [14].

The thin plate concept is applied in combination with a *p*-element to determine the first natural frequencies of symmetrically and antisymmetric laminated composite plates. The optimization of a curvilinear fiber cylindrical shell for improved buckling load is studied by Pitton et. al. [15]. A procedure in terms of AI methods is proposed. The paper defines an optimization procedure established for the buckling optimization of thin-walled curvilinear fiber cylindrical shells exposed to axial load. Ameri et. al. [16] offerings an optimization procedure for composite cylindrical panels for the first natural frequency. The Globalized Bounded Nelder–Mead method is applied to calculate the optimized fiber orientations of composite cylindrical shells to find the maximum natural frequency.

Maximization of first natural frequency by optimizing the path of fiber orientations is an extensively studied structural dynamic optimization problem [17–29].

This paper applies the Generalized Differential Quadrature (GDQ) method and virtual work rule to study the variation of the fundamental frequencies of variable stiffness, composite, doubly curved panels with CCCC and FCFC boundary conditions. The fundamental natural frequencies of curvilinear fiber composite, doubly curved panels are optimized. The optimum curvilinear fiber layups are identified by applying the genetic algorithm (GA) optimization method. The optimized fundamental natural frequencies are compared with the reference unidirectional fiber layup.

The Von-Karman strain-displacement relationship is employed in expressing the mathematical model of a doubly curved panel. The differential equation of motion of the composite, doubly curved panel is acquired applying the virtual work rule. Based on our earlier studies [20,21], spatial derivatives in the governing differential equation of motion are stated with the GDQ technique.

The present study is the first time of using a direct GA method in optimizing the fundamental natural frequencies of variable stiffness laminate doubly curved panels with different boundary conditions.

2. Governing Equation of Motions

The composite doubly curved rectangular planform panel is presumed to be as the schematic view given in Figure 2. Based on Figure 2, an orthogonal fixed coordinate system (x, y, z) is positioned at the root of the panel with a planform length a and b, and thickness h. The red lines represent the curved fiber path that is varied along the x-axis. θ is the angle that the curvilinear fibers create with the x-axis.

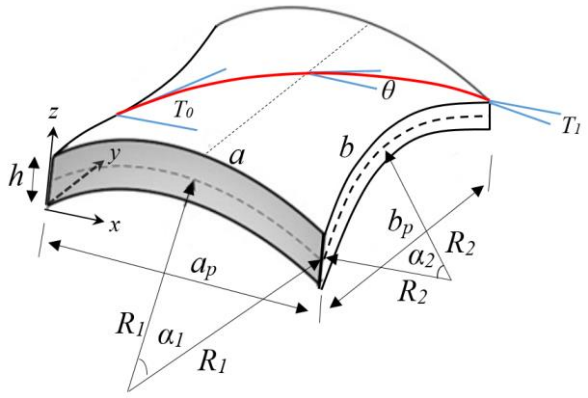

Figure 2 Composite doubly curved panel geometry and the curvilinear fiber path

The displacement domain of an arbitrary point (*x*, *y*, *z*) at time *t* on the panel (u, v, w) are indicated as,

$$\begin{aligned} u(x,y,z,t) &= u_0(x,y,t) + z\theta_x(x,y,t) \\ v(x,y,z,t) &= v_0(x,y,t) + z\theta_y(x,y,t) \\ w(x,y,z,t) &= w_0(x,y,t) \end{aligned} \tag{1}$$

where, u_0, v_0 and w_0 are the translations of mid-plane in the x, y and z direction, respectively and θ_x, θ_y are the rotations about the x, y axes. The strain-displacement relations are specified as following [20];

$$\varepsilon = \begin{Bmatrix} \varepsilon_x \\ \varepsilon_y \\ \gamma_{xy} \\ \gamma_{yz} \\ \gamma_{zx} \end{Bmatrix} = \begin{Bmatrix} \dfrac{\partial u_0}{\partial x} \\ \dfrac{\partial v_0}{\partial y} \\ \dfrac{\partial u_0}{\partial y} + \dfrac{\partial v_0}{\partial x} \\ \theta_y + \dfrac{\partial w_0}{\partial y} \\ \theta_x + \dfrac{\partial w_0}{\partial x} \end{Bmatrix} + z \begin{Bmatrix} \dfrac{\partial \theta_x}{\partial x} \\ \dfrac{\partial \theta_y}{\partial y} \\ \dfrac{\partial \theta_x}{\partial y} + \dfrac{\partial \theta_y}{\partial x} \\ 0 \\ 0 \end{Bmatrix} \tag{2}$$

In-plane moment and force resultants for a composite panel is obtained as, [20]

$$\begin{Bmatrix} N_x \\ N_y \\ N_{xy} \\ M_x \\ M_y \\ M_{xy} \end{Bmatrix} = \begin{bmatrix} A_{11} & A_{12} & A_{16} & B_{11} & B_{12} & B_{16} \\ A_{12} & A_{22} & A_{26} & B_{12} & B_{22} & B_{26} \\ A_{16} & A_{26} & A_{66} & B_{16} & B_{26} & B_{66} \\ B_{11} & B_{12} & B_{16} & D_{11} & D_{12} & D_{16} \\ B_{12} & B_{22} & B_{26} & D_{12} & D_{22} & D_{26} \\ B_{16} & B_{26} & B_{66} & D_{16} & D_{26} & D_{66} \end{bmatrix} \begin{Bmatrix} \dfrac{\partial u_0}{\partial x} + \dfrac{w_0}{R_1} \\ \dfrac{\partial v_0}{\partial y} + \dfrac{w_0}{R_2} \\ \dfrac{\partial u_0}{\partial y} + \dfrac{\partial v_0}{\partial x} \\ \dfrac{\partial \theta_x}{\partial x} \\ \dfrac{\partial \theta_y}{\partial y} \\ \dfrac{\partial \theta_x}{\partial y} + \dfrac{\partial \theta_y}{\partial x} \end{Bmatrix} \tag{3}$$

The formulations for transverse shear based on shear force resultant is expressed as,

$$\begin{Bmatrix} Q_y \\ Q_x \end{Bmatrix} = \begin{bmatrix} A_{44} & A_{45} \\ A_{45} & A_{55} \end{bmatrix} \begin{Bmatrix} \gamma_{yz} \\ \gamma_{zx} \end{Bmatrix} \tag{4}$$

where A_{ij}, B_{ij}, D_{ij} are stiffness coefficients of composite laminate for in-plane, bending stretching coupling, bending and transverse shear stiffness and are extracted as,

$$\left\{A_{ij},\, B_{ij},\, D_{ij}\right\} = \sum_{k=1}^{n} \int_{z_{k-1}}^{z_k} \left\{1,\, z,\, z^2\right\} \bar{Q}_{ij}^{(k)}\, dz \quad , \qquad i, j = 1, 2, 6 \tag{5}$$

$$A_{ij} = \sum_{k=1}^{n} k_i\, k_j \int_{z_{k-1}}^{z_k} \bar{Q}_{ij}^{(k)}\, dz \quad , \; i, j = 4, 5 \tag{6}$$

where k_i^2 is the shear correction factor and $\bar{Q}_{ij}^{(k)}$ is the *k*-th layer transformed stiffness quantities. Moment of inertia expression is detailed as:

$$\left\{I_0, I_1, I_2\right\} = \sum_{k=1}^{n} \int_{z_{k-1}}^{z_k} \left\{1, z, z^2\right\} \rho^{(k)} dz \tag{7}$$

where ρ is the layer density.

The equation for the composite laminated panel is expressed as [21],

$$\begin{aligned} &\sum_{k=1}^{L} \int_{z_{k-1}}^{z_k} [\int_{\Omega} \{\sigma_x^{(k)} \delta\varepsilon_x + \sigma_y^{(k)} \delta\varepsilon_y + \tau_{xy}^{(k)} \delta\gamma_{xy} + \\ &\tau_{yz}^{(k)} \delta\gamma_{yz} + \tau_{zx}^{(k)} \delta\gamma_{zx} \\ &\rho^{(k)} \begin{bmatrix} \left(\ddot{u}_0 + z\ddot{\theta}_x\right)\left(\delta u_0 + z\delta\theta_x\right) + \\ \left(\ddot{v}_0 + z\ddot{\theta}_y\right)\left(\delta v_0 + z\delta\theta_y\right) + \ddot{w}_0\, \delta w_0 \end{bmatrix} \} dxdy] dz \\ &= \int_{\Omega} p\, \delta w_0 dxdy \end{aligned} \tag{8}$$

where the p is the external work. Eq. (9) is reached by rephrasing the Eq. (8) based on the moment and force resultants:

$$\int_{\Omega}\begin{bmatrix} N_x\delta\varepsilon_x^0+N_y\delta\varepsilon_y^0+N_{xy}\delta\gamma_{xy}^0+M_x\delta\varepsilon_x^0+ \\ M_y\delta\varepsilon_y^0+M_{xy}\delta\gamma_{xy}^0+Q_y\delta\gamma_{yz}^0+Q_x\delta\gamma_{zx}^0+ \\ (I_0\ddot{u}_0+I_1\ddot{\theta}_x)\delta u_0+(I_0\ddot{v}_0+I_1\ddot{\theta}_y)\delta v_0+ \\ I_1\ddot{w}_0\,\delta w_0+(I_1\ddot{u}_0+I_2\ddot{\theta}_x)\delta\theta_x \\ +(I_1\ddot{v}_0+I_2\ddot{\theta}_y)\delta\theta_y \end{bmatrix} dxdy \tag{9}$$

$$=\int_{\Omega} p\,\delta w_0 dxdy$$

Based on our previous research [20, 21], geometric mapping is considered for numerical integral calculations. By applying the suggested mapping method, the Cartesian domain is converted into a bi-unit square domain.

3. Generalized Differential Quadrature Method

Based on the generalized differential quadrature method, *r*-th order derivative of a function *f(ξ)* with *n* discrete grid points may be defined as:

$$\left(\frac{\partial f^r(x)}{\partial\xi^r}\right)_{\xi_i}=\sum_{j=1}^{n}C_{ij}^{(r)}f_j \tag{10}$$

where ξ_i are discrete points in the domain and $C_{ij}^{(r)}$, f_j are weighting parameters and function values at points, respectively. An obvious formulation for the weight parameters in terms of Lagrange polynomial formulation for first-order derivative, i.e. r =1, is as the following:

$$C_{ij}^{(1)}=\frac{\Phi(\xi_i)}{(\xi_i-\xi_j)\Phi(\xi_j)} \qquad (i\neq j) \tag{11}$$

Where

$$\Phi(\xi_i)=\prod_{j=1}^{n}(\xi_i-\xi_j) \qquad (i\neq j) \tag{12}$$

The subsequent recursive relationships are utilized for higher-order derivatives:

$$C_{ij}^{(r)}=r\left[C_{ii}^{(r-1)}C_{ij}^{(1)}-\frac{C_{ij}^{(r-1)}}{(\xi_i-\xi_j)}\right] \qquad (i\neq j) \tag{13}$$

$$C_{ii}^{(r)}=-\sum_{\substack{j=1\\ i\neq j}}^{n}C_{ij}^{(r)} \tag{14}$$

Based on Figure 3 partial derivates at a point (ξ_i,η_j) are expressed as follows, where n_ξ and n_η represent grid numbers in ξ and η direction, respectively:

$$\left(\frac{\partial f^r(\xi,\eta)}{\partial\xi^r}\right)_{\xi_i,\eta_j}=\sum_{k=1}^{n_x}C_{kj}^{(r)}f_{kj} \tag{15}$$

$$\left(\frac{\partial f^s(\xi,\eta)}{\partial\eta^s}\right)_{\xi_i,\eta_j}=\sum_{m=1}^{n_y}C_{im}^{(s)}f_{im} \tag{16}$$

$$\left(\frac{\partial f^{(r+s)}(\xi,\eta)}{\partial\xi^r\partial\eta^s}\right)_{\xi_i,y_j}=\frac{\partial^r}{\partial\xi^r}\left(\frac{\partial^s f}{\partial\eta^s}\right)=\sum_{k=1}^{n_x}C_{kj}^{(r)}\sum_{m=1}^{n_y}C_{im}^{(s)}f_{km} \tag{17}$$

where r and s represent derivative orders respecting the variables ξ and η, respectively.

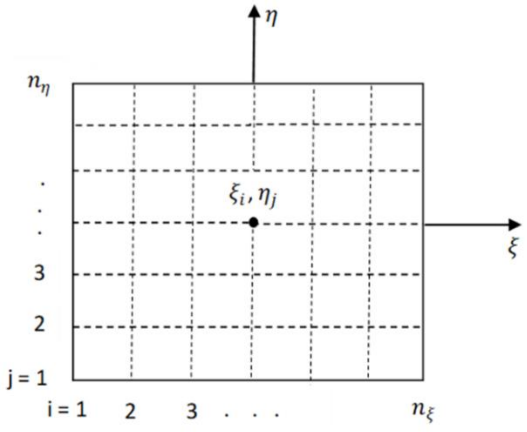

Figure 3 Mesh grid scheme

In Eqs. (15)-(17), the partial derivatives $\partial f/\partial\xi$ and $\partial f/\partial\eta$ are obtained utilizing DQM at grid point;

$$\left(\frac{\partial f}{\partial x}\right)_{ij}=\frac{1}{J_{ij}}\left[\left(\frac{\partial y}{\partial\eta}\right)_{ij}\left(\sum_{k=1}^{n_x}C_{kj}^{(1)}f_{kj}\right)-\left(\frac{\partial y}{\partial\xi}\right)_{ij}\left(\sum_{m=1}^{n_y}C_{im}^{(1)}f_{im}\right)\right] \tag{18}$$

$$\left(\frac{\partial f}{\partial y}\right)_{ij}=\frac{1}{J_{ij}}\left[\left(\frac{\partial x}{\partial\xi}\right)_{ij}\left(\sum_{m=1}^{n_y}C_{im}^{(1)}f_{im}\right)-\left(\frac{\partial x}{\partial\eta}\right)_{ij}\left(\sum_{k=1}^{n_x}C_{kj}^{(1)}f_{kj}\right)\right] \tag{19}$$

4. Solution Methodology

In order to solve an eigenvalue problem for the frequency study of the doubly curved panel, the external force in Eq. (9) is omitted. By discretizing the panel domain into grid points and utilizing GDQ theory for computing partial derivatives at each grid point, and Gauss-Lobatto quadrature principle, it can be possible to calculate the integrals in virtual work. The matrix form of the equation of motion can be stated as,

$$\mathbf{M}\ddot{\mathbf{U}} + \mathbf{K}\mathbf{U} = 0 \tag{20}$$

where **M** specifies the mass matrix and $\ddot{\mathbf{U}}$, **K** express the acceleration vectors and stiffness matrix, respectively.

5. Variable Stiffness Description

Figure 4 demonstrates the VSCL configuration presented by curvilinear fiber path functions. The functions of fiber path variation for each layup shape is presented in Eq. (21). The two design parameters T_0 and T_1 are essential to control the change of the fiber angle on the surface of the lamina.

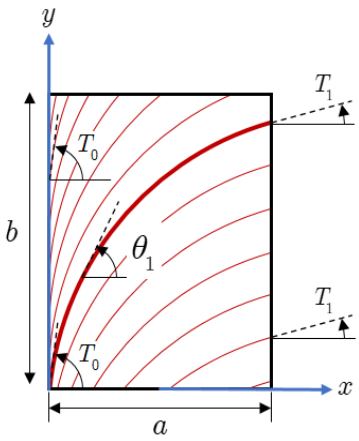

Figure 4 Curvilinear fiber paths

For VSCL;

$$\theta \rightarrow \langle T_0, T_1 \rangle = T_0 + \left(T_1 - T_0\right)\left(\frac{x}{a_p}\right) \tag{21}$$

Where

$$a_p = 2R\sin\left(\frac{a}{2R}\right) \tag{22}$$

6. Optimization Strategy

The goal of the optimization strategy is to maximize the first (fundamental) natural frequency of the doubly curved panel by optimizing the fiber path function. The stacking scheme for the present eight layers composite doubly curved panel is in the form of Eq. (23) and shown in Figure 5,

$$\left[\theta_1 / \theta_2 / -\theta_3 / -\theta_4\right]_{sym} \rightarrow \left[\left\langle T_0^{L1}, T_1^{L1}\right\rangle / \left\langle T_0^{L2}, T_1^{L2}\right\rangle / -\left\langle T_0^{L3}, T_1^{L3}\right\rangle / -\left\langle T_0^{L4}, T_1^{L4}\right\rangle\right]_{sym} \tag{23}$$

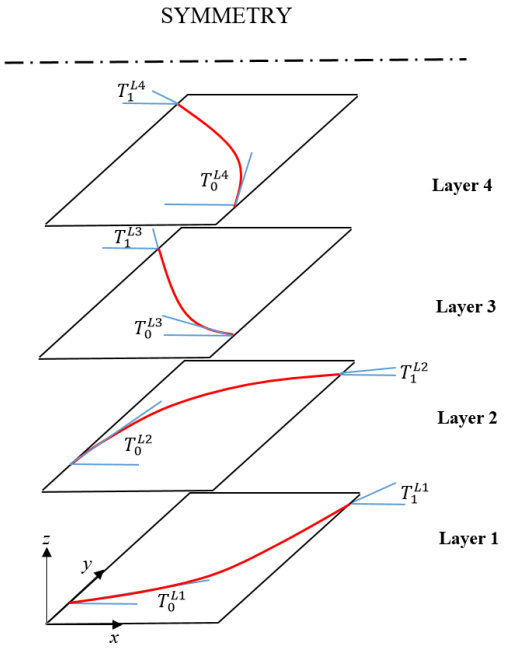

Figure 5 Stacking scheme for present eight layers composite cylindrical curved panel

In the recommended optimization tactic, the composite doubly curved panel fundamental frequency is maximized. The cost function in the procedure is the fundamental frequency and the variables are improved to catch the maximized value of the first natural frequency.

The start fiber angle (T_0) and the final fiber angle (T_1) are the variables considered in the optimization procedure. The following are the definitions of the objective, constraints and variables in the present optimization procedure.

Objective Fundamental Natural Frequency → Maximum

Constraints For each layer [7]

$$\frac{(T_1 - T_0)}{a}\cos\left((T_1 - T_0)\frac{x}{a} + T_0\right) < 3.28$$

Optimum Variables

$$0^\circ \le T_0^{L1} \le 45^\circ, \quad 0^\circ \le T_1^{L1} \le 90^\circ$$
$$45^\circ \le T_0^{L2} \le 90^\circ, \quad 0^\circ \le T_1^{L2} \le 90^\circ$$
$$0^\circ \le T_0^{L3} \le 45^\circ, \quad 0^\circ \le T_1^{L3} \le 90^\circ$$
$$45^\circ \le T_0^{L4} \le 90^\circ, \quad 0^\circ \le T_1^{L4} \le 90^\circ$$

After introducing and expressing the variables, constraints, and cost function of the optimization method, genetic algorithm (GA) [22] is considered to optimize the solutions. The GA MATLAB code is developed with the maximum number of generations of 200 and the population size of 110.

7. Numerical Results

The natural frequency optimization consequences are determined by utilizing the equations obtained for the composite doubly curved panel. The convergence study displays that a minimum number of elements in *x,y,* and *z* directions *(n_x, n_y, n_z)* = (13, 13, 5) is essential to offer a solid convergence. The accuracy of the developed computer code is judged by the following validation studies.

7.1. Structural Model Validation

To endorse the curvilinear fiber model, the natural frequencies of the variable stiffness plate are compared with the outcomes of Ref. [23] in Table 1. Table 1 displays the assessment of frequencies for SSSS and CCCC boundary conditions of the variable stiffness composite lamina and fiber path angles produced by $\langle T_0, T_1 \rangle$.

Table 1 Comparison of natural frequencies of VSCL with curvilinear fibers

VSCL plate	Method	Mode 1	Mode 2	Mode 3
		$[\langle 0,45\rangle / \langle -45,60\rangle / \langle 0,45\rangle]$		
Simply supported	Ref [23]	358.488	589.9	960.361
	Present study	351.622	581.41	954.14
Clamped	Ref [23]	579.398	821.532	1225.79
	Present study	579.745	822.601	1227.56
		$[\langle 30,0\rangle / \langle 45,90\rangle / \langle 30,0\rangle]$		
Simply supported	Ref [23]	308.799	503.799	845.509
	Present study	307.62	504.11	846.79
Clamped	Ref [23]	667.177	862.919	1234.64
	Present study	665.217	863.689	1238.5
		$[\langle 90,45\rangle / \langle 60,30\rangle / \langle 90,45\rangle]$		
Simply supported	Ref [23]	329.688	539.407	886.392
	Present study	323.99	533.1	880.587
Clamped	Ref [23]	710.77	912.183	1335.49
	Present study	709.46	915.47	1340.98

To validate the curved panel structural model, Table 2 shows the fundamental natural frequencies computed with Ref [24] for cylindrical panel model with *ap/R* = 0.4, 0.2 with *h* = 1 mm and *ap/R* = 0.4, 0.2 with *h* = 2.5 mm. The material properties are E=7 $\times 10^{10}$ Nm^{-2}, υ = 0.33, ρ = 2778 kg m^{-3}

Table 2 Comparison of first and second natural frequencies (rad/s) of a cylindrical panel structure

		ap/R = 0.4 *h* = 1 mm	*ap/R* = 0.2 *h* = 1 mm	*ap/R* = 0.4 *h* = 2.5 mm	*ap/R* = 0.2 *h* = 2.5 mm
fundamental mode	Ref [24]	1137.61	865.359	2044.97	1662.75
	Present study	1136.76	864.25	2036.16	1660

7.2. Results and Discussion

The results section is separated into two sub-sections. First, the frequency behavior of the doubly curved panel with rectangular planform and CCCC boundary condition is studied. Second, the doubly curved panel with FCFC boundary conditions is considered in frequency analysis. In each sub-sections, the natural frequencies of the composite panels are maximized for the different boundary conditions by determining optimum fiber path angles by applying the GA algorithm. The stacking scheme for the present eight layers composite cylindrical curved panel with *curvilinear fiber path* is given in Eq. (23). The reference conventional *unidirectional layup sequence* for the sake of comparison is considered to be in the form of,

$$\left[\theta_1 / \theta_2 / -\theta_3 / -\theta_4\right]_{sym} \rightarrow \left[0 / 45 / -90 / -45\right]_{sym} \quad (24)$$

Composite cylindrical panel geometries along with material characteristics are given in Table 3 based on the parameters defined in Table 3.

Table 3 Geometric and material properties

a=b=1 (m)	*E2=7.2 (GPa)*	*G23=3.76 (GPa)*
h=a/100	*G12=3.76 (GPa)*	υ_{12} *=0.29*
E1=173 (GPa)	*G13=3.76 (GPa)*	ρ $\left(\mathrm{kg/m^3}\right)$ *=1540*

In the first sub-section, the first natural frequency of rectangular planform curved panel is maximized by curvilinear fiber concept using Genetic Algorithm (GA). For this aim, fiber angles ($T_0^{Li}, T_1^{Li}, i = 1,2,3,4$) for each composite layer are varied to achieve the best values. Due to symmetry in composite layers, fiber angles of the first four layers are considered in the optimization process. Figure 6a-f illustrate the optimum variables of curvilinear fiber path parameters ($T_0^{Li}, T_1^{Li}, i = 1,2,3,4$) for four layers of the preferred doubly curved panel, as well as the maximum reachable natural frequencies using the optimum parameters deduced by optimization algorithm for doubly curved panel with curvature radius ratios of $\frac{R_1}{a} = 2, 10, \infty$ and $\frac{R_2}{b} = 2, 10, \infty$ for fully clamped rectangular panel, respectively. After the 10th generation, the fitness starts to converge to the optimal cost. Table 4 compares the result of the maximum fundamental natural frequency of the VSCL composite panel calculated via optimization and unidirectional composite panel as a reference conventional configuration to prove the advantages of the variable stiffness concept. Table 4 gives the optimized layup sequence of the VSCL composite panel and the associated natural frequencies for different curvature radius ratios. The following results are deduced.

The optimum fiber paths of the layers are diverse for VSCL panels with different width and length curvature radius ratios. With an increase in curvature radius ratios both in width and length dimensions from $\frac{R_1}{a}, \frac{R_2}{b} = 2$ to $\frac{R_1}{a}, \frac{R_2}{b} = \infty$ (as a flat plate), maximum fundamental natural frequency continuously decreasing. This trend is seen in both VSCL and unidirectional reference panels. The maximum fundamental natural frequency is achieved in VSCL panels with close to zero deg fiber angles in the first layer ($T_0^{L1} = T_1^{L1} \approx 0^\circ$) in almost all case studies except $\frac{R_1}{a}, \frac{R_2}{b} = 2$ which has ($T_0^{L3} = 10^\circ, T_1^{L3} = 34^\circ$) in the first layer. The first layer is the layer with the highest distance from the neutral axis. The first layer and eighth layer are the same due to symmetry. By increasing the length curvature radius ratio $\frac{R_2}{b}$ and constant width ratio $\frac{R_1}{a}$, the second and the fourth layers in VSCL panels are very effective in achieving the highest fundamental frequencies. Larger initial fiber T_0^{L2}, T_0^{L4} and smaller final angles T_1^{L2}, T_1^{L4} are desirable. The highest advantages of applying VSCL concept is seen for panel with $\frac{R_1}{a}, \frac{R_2}{b} = 2,2$ and $\frac{R_1}{a}, \frac{R_2}{b} = 10, \infty$ with different percentages of 16% and 15.1%, respectively. The lowest advantages are seen for high curvature radius ratios $\frac{R_1}{a}, \frac{R_2}{b} = 10,10$ and $\frac{R_1}{a}, \frac{R_2}{b} = \infty, \infty$. It shows that the variable stiffness concept is more advantageous in low curved panels rather than high curved panels especially plates with fully clamped BCs.

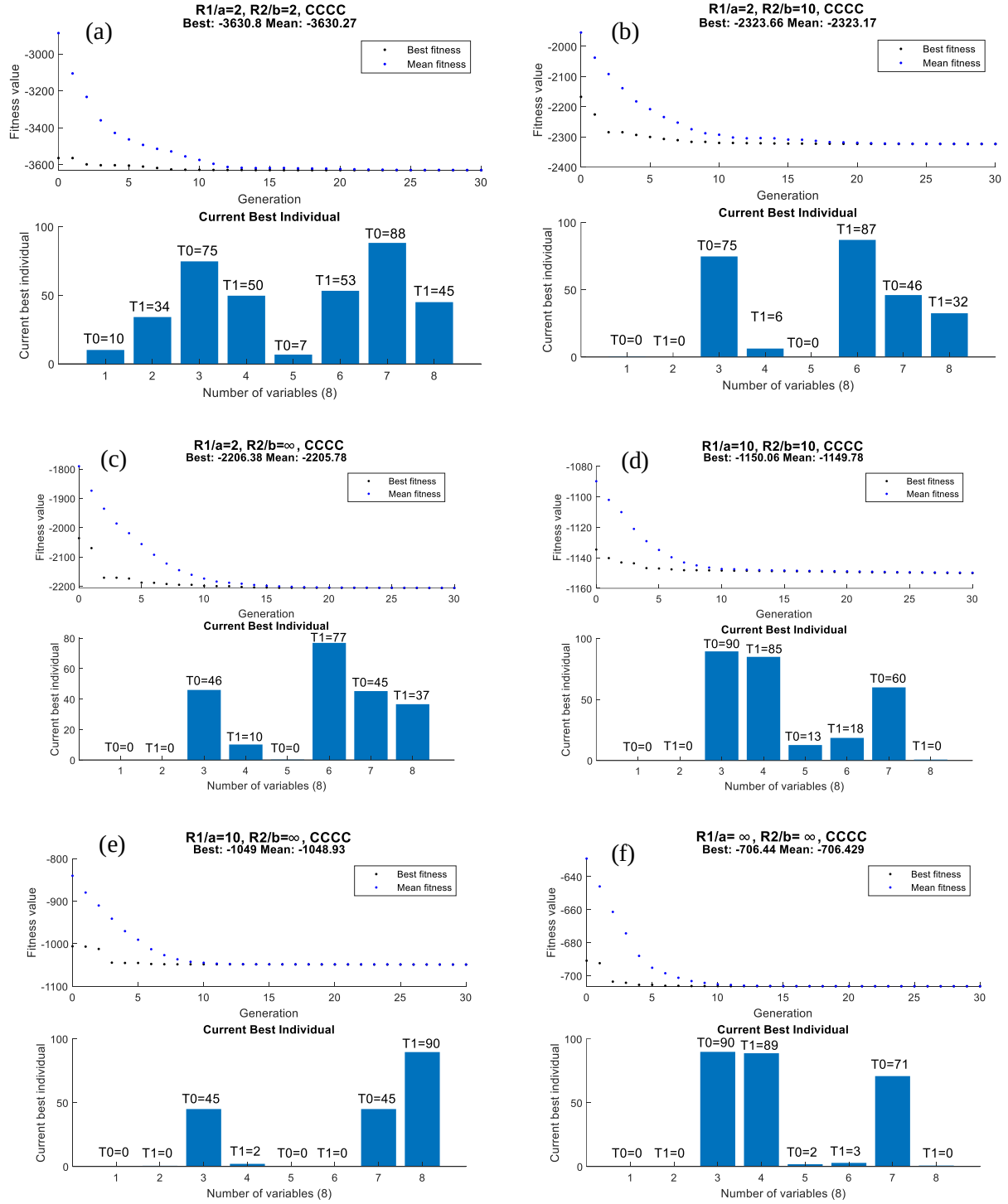

Figure 6 Fundamental frequency optimization of doubly curved panel with CCCC BCs,
a) $R_1/a=2$, $R_2/b=2$, b) $R_1/a=2$, $R_2/b=10$, c) $R_1/a=2$, $R_2/b=\infty$,
d) $R_1/a=10$, $R_2/b=10$, e) $R_1/a=10$, $R_2/b=\infty$ and f) $R_1/a=\infty$, $R_2/b=\infty$

Table 4 Comparisons of the natural frequency of optimized curvilinear fiber and unidirectional fiber for rectangular CCCC panels

$\frac{R_1}{a}, \frac{R_2}{b}$	Max fundamental frequency with curvilinear fiber path	Max fundamental frequency with Unidirectional layups	Nat. Freq. Diff.
2, 2	$\left[\langle 10,34\rangle / \langle 75,50\rangle / -\langle 0,53\rangle / -\langle 88,45\rangle\right]_{sym}$ ω = 3630.8 rad/sec	$\left[0 / 45 / -90 / -45\right]_{sym}$ ω = 3052.7 rad/sec	16 %
2,10	$\left[\langle 0,0\rangle / \langle 75,6\rangle / -\langle 0,87\rangle / -\langle 46,32\rangle\right]_{sym}$ ω = 2323.6 rad/sec	$\left[0 / 45 / -90 / -45\right]_{sym}$ ω =2137.2 rad/sec	8.1 %
2, ∞	$\left[\langle 0,0\rangle, \langle 46,10\rangle, -\langle 0,77\rangle, -\langle 45,37\rangle\right]_{sym}$ ω = 2206.4 rad/sec	$\left[0 / 45 / -90 / -45\right]_{sym}$ ω = 1997.7 rad/sec	9.5 %
10, 10	$\left[\langle 0,0\rangle, \langle 90,85\rangle, -\langle 13,18\rangle, -\langle 60,0\rangle\right]_{sym}$ ω = 1150 rad/sec	$\left[0 / 45 / -90 / -45\right]_{sym}$ ω = 1131.1 rad/sec	1.7 %
10, ∞	$\left[\langle 0,0\rangle, \langle 45,2\rangle, -\langle 0,0\rangle, -\langle 45,90\rangle\right]_{sym}$ ω = 1049 rad/sec	$\left[0 / 45 / -90 / -45\right]_{sym}$ ω = 891.1 rad/sec	15.1 %
∞, ∞	$\left[\langle 0,0\rangle, \langle 90,89\rangle, -\langle 2,3\rangle, -\langle 71,0\rangle\right]_{sym}$ ω = 706.44 rad/sec	$\left[0 / 45 / -90 / -45\right]_{sym}$ ω = 689.7 rad/sec	2.37 %

In the second sub-section, the optimization results are given to investigate the effects of the VSCL concept on the fundamental natural frequency of doubly curved panels with different width and length curvature radius ratios and FCFC BCs. In Figure 7 and Table 5 It is found out that;
In the same manner with fully clamped panel configuration, by increasing the curvature radius ratio maximum fundamental natural frequency constantly decreasing for both VASL and unidirectional concepts. The trend is the same for both CCCC and FCFC BCs.

The maximum fundamental natural frequency is achieved in VSCL panels and FCFC BCs. with a constant fiber path angle of zero deg ($T_0^{L1} = T_1^{L1} = 0^\circ$) in the first layer and ($T_0^{L2} = 45^\circ$, $T_1^{L2} \approx 0^\circ$) in the second layer in almost all case studies. The two layers with the highest distance from the neutral axis.

It is found that the VSCL concept in panels with high curvature radius ratios $\frac{R_1}{a}, \frac{R_2}{b} = 10, \infty$ and $\frac{R_1}{a}, \frac{R_2}{b} = 10,10$ gives the highest difference percentages 22.3% and 19.5% in frequency values over the unidirectional concept, respectively.

Comparing the effect of the VSCL concept in different BCs. for fundamental natural frequency shows that FCFC BCs. gives the greater advantages over the fully clamped BCs.

This type of composite optimization method could be applied in various kinds of plate geometries and configurations [25-27] to improve the mechanical performance of the structures.

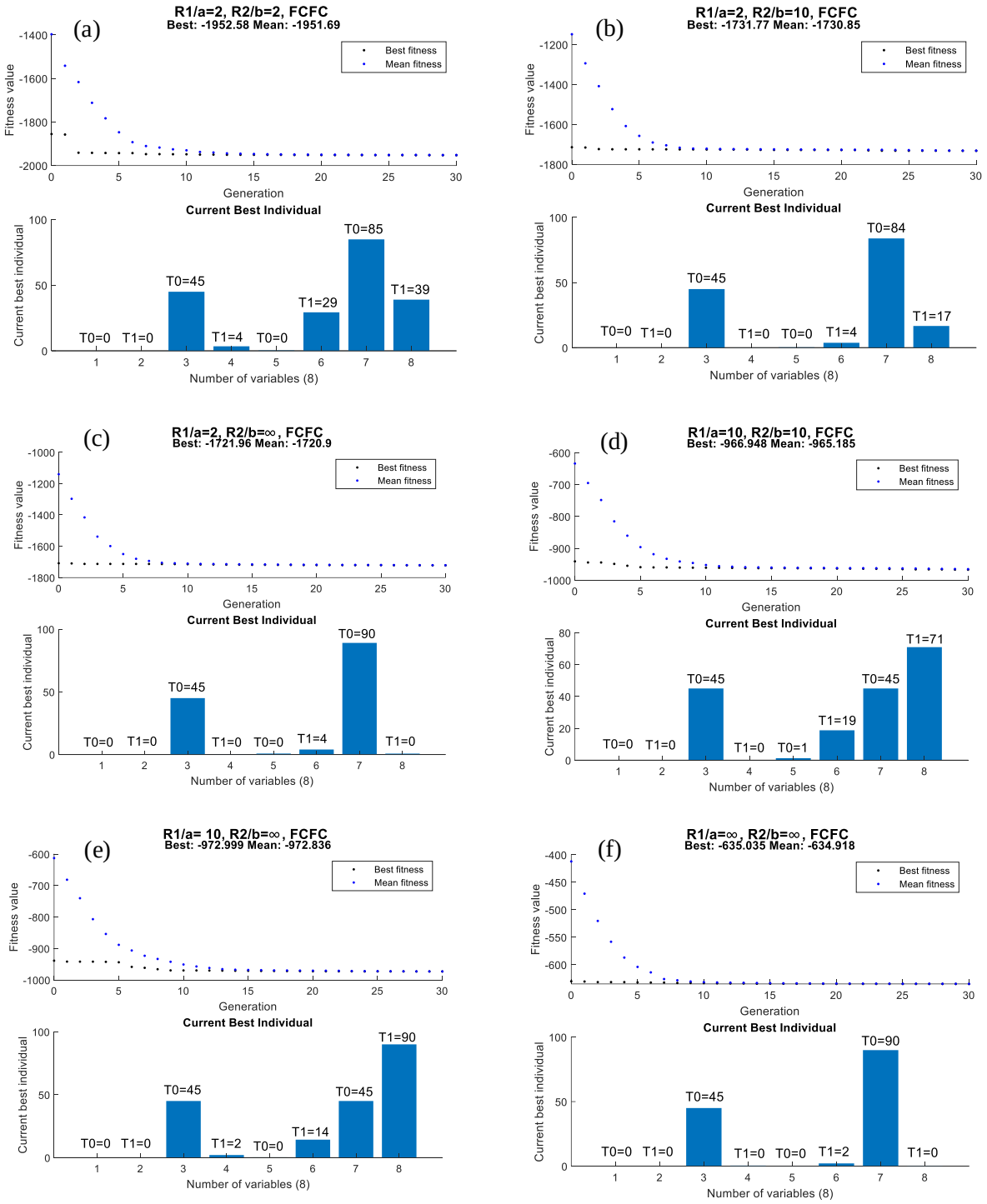

Figure 7 Fundamental frequency optimization of doubly curved panel with FCFC BCs, a) $R_1/a=2$, $R_2/b=2$, b) $R_1/a=2$, $R_2/b=10$, c) $R_1/a=2$, $R_2/b=\infty$, d) $R_1/a=10$, $R_2/b=10$, e) $R_1/a=10$, $R_2/b=\infty$ and f) $R_1/a=\infty$, $R_2/b=\infty$

Table 5 Comparisons of natural frequency of optimized curvilinear fiber and unidirectional fiber for rectangular FCFC panels

$\frac{R_1}{a}, \frac{R_2}{b}$	Max fundamental frequency with curvilinear fiber path	Max fundamental frequency with Unidirectional layups	Nat. Freq. Diff.
2, 2	$\left[\langle 0,0\rangle / \langle 45,4\rangle / -\langle 0,29\rangle / -\langle 85,39\rangle\right]_{sym}$ $\omega_{nat.}$ = 1952.6 rad/sec	$\left[0 / 45 / -90 / -45\right]_{sym}$ $\omega_{nat.}$ = 1789.5 rad/sec	8.35 %
2,10	$\left[\langle 0,0\rangle / \langle 45,0\rangle / -\langle 0,4\rangle / -\langle 84,17\rangle\right]_{sym}$ ω = 1730.7 rad/sec	$\left[0 / 45 / -90 / -45\right]_{sym}$ ω = 1513.7 rad/sec	12.5 %
2, ∞	$\left[\langle 0,0\rangle, \langle 45,0\rangle, -\langle 0,4\rangle, -\langle 90,0\rangle\right]_{sym}$ ω = 1721.9 rad/sec	$\left[0 / 45 / -90 / -45\right]_{sym}$ ω = 1495 rad/sec	13.2 %
10, 10	$\left[\langle 0,0\rangle, \langle 45,0\rangle, -\langle 1,19\rangle, -\langle 45,71\rangle\right]_{sym}$ ω = 966.9 rad/sec	$\left[0 / 45 / -90 / -45\right]_{sym}$ ω = 777.7 rad/sec	19.5 %
10, ∞	$\left[\langle 0,0\rangle, \langle 45,2\rangle, -\langle 0,14\rangle, -\langle 45,90\rangle\right]_{sym}$ ω = 972.8 rad/sec	$\left[0 / 45 / -90 / -45\right]_{sym}$ ω = 755.7 rad/sec	22.3 %
∞, ∞	$\left[\langle 0,0\rangle, \langle 45,0\rangle, -\langle 0,2\rangle, -\langle 90,0\rangle\right]_{sym}$ ω = 635 rad/sec	$\left[0 / 45 / -90 / -45\right]_{sym}$ ω = 551.5 rad/sec	13.15 %

Conclusion

In the present study, the influence of fiber path function on free vibration of VSCL composite doubly curved panel is examined for two forms of boundary conditions. The GDQ method and Hamilton's principle are applied to study the variation of the fundamental frequencies of the variable stiffness composite panels. The genetic algorithm is applied to optimize the fundamental natural frequencies of curvilinear fiber composite panels. Genetic algorithm in a nonlinear constraint optimization problem is utilized to derive the optimum fiber angle orientation of each layer in an eight-layer variable stiffness panel.

Ethical Approval

Not applicable.

References

[1] Abdalla, M. M., Setoodeh, S., & Gürdal, Z. (2007). Design of variable stiffness composite panels for maximum fundamental frequency using lamination parameters. Composite structures, 81(2), 283-291.

[2] Labans, E., & Bisagni, C. (2019). Buckling and free vibration study of variable and constant-stiffness cylindrical shells. Composite Structures, 210, 446-457.

[3] Narita, Y., & Robinson, P. (2006). Maximizing the fundamental frequency of laminated cylindrical panels using layerwise optimization. International Journal of Mechanical Sciences, 48(12), 1516-1524.

[4] Serhat, G., & Basdogan, I. (2019). Lamination parameter interpolation method for design of manufacturable variable-stiffness composite panels. AIAA Journal, 3052-3065.

[5] Blom AW. Structural performance of fiber-placed, variable-stiffness composite conical and cylindrical shells. PhD Thesis, Faculty of Aerospace Engineering, Delft University of Technology, Delft, The Netherlands, 2010.

[6] Blom, A. W., Stickler, P. B., & Gürdal, Z. (2010). Optimization of a composite cylinder under bending by tailoring stiffness properties in circumferential direction. Composites Part B: Engineering, 41(2), 157-165.

[7] Blom, A. W., Setoodeh, S., Hol, J. M., & Gürdal, Z. (2008). Design of variable-stiffness conical shells for maximum fundamental eigenfrequency. Computers & structures, 86(9), 870-878.

[8] Honda, S., Igarashi, T., & Narita, Y. (2013). Multi-objective optimization of curvilinear fiber shapes for laminated composite plates by using NSGA-II. Composites Part B: Engineering, 45(1), 1071-1078.

[9] Tornabene, F., Fantuzzi, N., Bacciocchi, M., & Viola, E. (2015). Higher-order theories for the free vibrations of doubly-curved laminated panels with curvilinear reinforcing fibers by means of a local version of the GDQ method. Composites Part B: Engineering, 81, 196-230.

[10] Zhao, W., & Kapania, R. K. (2019). Prestressed vibration of stiffened variable-angle tow laminated plates. AIAA Journal, 57(6), 2575-2593.

[11] Wu, C. P., & Lee, C. Y. (2001). Differential quadrature solution for the free vibration analysis of laminated conical shells with variable stiffness. International Journal of Mechanical Sciences, 43(8), 1853-1869.

[12] Luersen, M. A., Steeves, C. A., & Nair, P. B. (2015). Curved fiber paths optimization of a composite cylindrical shell via Kriging-based approach. Journal of Composite Materials, 49(29), 3583-3597.

[13] Hao, P., Yuan, X., Liu, C., Wang, B., Liu, H., Li, G., & Niu, F. (2018). An integrated framework of exact modeling, isogeometric analysis and optimization for variable-stiffness composite panels. Computer Methods in Applied Mechanics and Engineering, 339, 205-238.

[14] Houmat, A. (2018). Optimal lay-up design of variable stiffness laminated composite plates by a layer-wise optimization technique. Engineering Optimization, 50(2), 205-217.

[15] Pitton, S. F., Ricci, S., & Bisagni, C. (2019). Buckling optimization of variable stiffness cylindrical shells through artificial intelligence techniques. Composite Structures, 230, 111513.

[16] Ameri, E., Aghdam, M. M., & Shakeri, M. (2012). Global optimization of laminated cylindrical panels based on fundamental natural frequency. Composite Structures, 94(9), 2697-2705.

[17] Koide, R. M., & Luersen, M. A. (2013). Maximization of fundamental frequency of laminated composite cylindrical shells by ant colony algorithm. Journal of Aerospace Technology and Management, 5(1), 75-82.

[18] Farsadi, T., Asadi, D., & Kurtaran, H. (2020). Fundamental frequency optimization of variable stiffness composite skew plates. Acta Mechanica, 1-19.

[19] Ghashochi-Bargh, H., & Sadr, M. H. (2013). PSO algorithm for fundamental frequency optimization of fiber metal laminated panels. Structural Engineering and Mechanics, 47(5), 713-727.

[20] Farsadi, T., Rahmanian, M., & Kurtaran, H. Nonlinear analysis of functionally graded skewed and tapered wing-like plates including porosities: A bifurcation study. Thin-Walled Structures, 160, 107341.

[21] Farsadi, T., Asadi, D., & Kurtaran, H. (2020). Nonlinear flutter response of a composite plate applying curvilinear fiber paths. Acta Mechanica, 231(2), 715-731.

[22] Song, Z. G., & Li, F. M. (2014). Optimal locations of piezoelectric actuators and sensors for supersonic flutter control of composite laminated panels. Journal of Vibration and Control, 20(14), 2118-2132.

[23] Akhavan, H., & Ribeiro, P. (2011). Natural modes of vibration of variable stiffness composite laminates with curvilinear fibers. Composite Structures, 93(11), 3040-3047.

[24] Ribeiro, P. (2008). Non-linear free periodic vibrations of open cylindrical shallow shells. Journal of sound and vibration, 313(1-2), 224-245.

[25] Javanshir, J., Farsadi, T., & Yuceoglu, U. (2012). Free vibrations of composite base plates stiffened by two adhesively bonded plate strips. Journal of aircraft, 49(4), 1135-1152.

[26] Javanshir, J., Farsadi, T., & Yuceoglu, U. (2014). Free flexural vibration response of integrally-stiffened and/or stepped-thickness composite plates or panels. Int J Acoust Vib, 19(2), 114-126.

[27] Farsadi, T., Heydarnia, E., & Amani, P. (2012). Buckling behavior of composite triangular plates. A A, 1(2), 3.